Electronic Supplementary Material (ESI) for Soft Matter.

Supporting Information

Mechanism of adhesion and graft polymerization of PNIPAAm thermoresponsive hydrogel to polypropylene meshes

Sonia Lanzalaco,[a,b,§] Pau Turon,[c] Christine Weis,[c] Carlos Alemán,[a,b] Elaine Armelin[a,b,§]

[a] *Departament d'Enginyeria Química, EEBE, Universitat Politècnica de Catalunya, C/ Eduard Maristany, 10-14, Ed. I.2, 08019, Barcelona, Spain.*

[b] *Barcelona Research Center for Multiscale Science and Engineering, Universitat Politècnica de Catalunya, C/ Eduard Maristany, 10-14, Ed. I.S, 08019, Barcelona, Spain.*

[c] *B. Braun Surgical, S.A. Carretera de Terrassa 121, 08191 Rubí (Barcelona), Spain.*

[§] Corresponding authors: elaine.armelin@upc.edu and sonia.lanzalaco@upc.edu

2. Experimental section

2.4. Physical-chemical characterization

Raman spectroscopy was also used to estimate the crystallinity (X_C) and the degree of isotacticity of iPP matrix before and after plasma functionalization. In order to ascertain the relationship between the crystalline phases in the iPP molecular chain, with *trans–gauche* conformation, at 809 cm^{-1}, and the amorphous-phases detected at 841 cm^{-1}, the crystallinity was calculated using the approach reported by Galiotis and co-workers:[1]

$$Cristallinity = \frac{I_{809}}{I_{809}+I_{841}} \quad (1)$$

where I_{809} and I_{841} are the intensities of scattering bands located at 809 and 841 cm^{-1}, respectively. However, the crystallinity index deduced from Eq (1) is based on the intensity of scattering bands that are not pure crystalline (809 cm^{-1}, 60% of crystallinity; 841 cm^{-1}, 65% of crystallinity) and, therefore, one correction is necessary. Bourson and co-workers [2] proposed the following equation for the crystallinity measurements on PP matrices (X_C):

$$X_c = 0.81 \times Cristallinity + 0.01 \quad (2)$$

The isotacticity was calculated by Eq. (3), according to Sundell and co-workers:[3]

$$Isotacticity = \frac{I_{809}}{I_{973}} \quad (3)$$

2.6. Volume phase transition temperature (VPTT) of the bilayer system

The graft yield (GY, in mg/cm^2) of the iPP-*g*-PNIPAAm samples was evaluated from the weight increases after the graft polymerization. The grafting amount of PNIPAAm on the treated PP mesh was calculated as follows (Eq. 4):

$$GY = \frac{W_f - W_0}{A} \quad (4)$$

where W_f and W_o represent the weight of the mesh after and before grafting, respectively, while A is the area of iPP mesh.

The equilibrated swelling ratio (ESR, in %) of the PNIPAAm gel covalently bonded to iPP mesh was obtained after the immersion of iPP-*g*-PNIPAAm samples in 10 mL of milli-Q water for 24 hours at 25 °C. After removal from vessel and elimination of the water in excess, the ESR was measured using the following Eq. (5):

$$ESR = \frac{W_s - W_d}{W_d} \times 100 \quad (5)$$

where W_s and W_d are the weights of swollen and dry gel, respectively. The accuracy of the measurements was 3%. All measurements were performed in triplicate.

3. Results and discussion

3.2. Effect of the purging pressure and plasma power in the surface functionalization of polypropylene mesh

The variation of the O 1s atomic concentration, which is related to the amount of oxidized functional groups (C–O, C=O and O–C=O), with the operational conditions is shown in Table S1. More in detail, the amount of O–C=O functional group increases with the purging pressure value. As it was expected, the interaction of the polymer surface with the plasma causes the rupture of C–H linkages from polymeric chains and the creation of free radicals. Those radicals, induced by the plasma activation, interact with oxygen and, hence, new functional groups are incorporated onto the polymer surface that becomes very active. XPS results suggest that the nature of reactive species formed upon exposure of the iPP mesh to the plasma depends on the amount of air present after the purging step. The ratio O_2/air inside the equipment depends on the time of the vacuum purging (*i.e.* high pressure values means less time of vacuum purging). Before applying plasma, the longer time of vacuum step investigated in this work (0.070 mbar) led to higher atomic concentrations of oxygen species on the iPP surface than the higher purging pressure used (0.20 mbar) or than the pristine polymer (Table S1). However, the composition of oxygen functional groups (C=O, C–O, O–C=O) upper iPP fibres almost does not change. As for example, the amount of O–C=O species are 20.16 ± 1.74 and 19.49 ± 0.42 for 0.20 mbar and 0.07 mbar, respectively.

Table S2 show the O/C atomic ratio when comparing the samples without plasma treatment and samples treated with variable purging down pressure.

Table S1. Atomic concentration of C 1s and O 1s of Optilene® mesh before and after plasma activation at constant plasma power discharge (500W) and time (180s), and with variable purging down pressures.[a)]

Sample code	Pressure (mbar)	Element	Atomic concentration (%)	Functional group	Binding energy (eV)	Oxygen concentration[b)] (%)
Pristine Optilene® mesh LP	-	C 1s	98.28 ± 0.57	O 1s (C=O)	533.6	30.10 ± 0.19
		O 1s	1.72 ± 0.57	O 1s (C–O)	532.2	69.90 ± 0.19
Sample 1	0.20	C 1s	79.01 ± 0.14	O 1s (C=O)	534.3	58.83 ± 1.14
		O 1s	20.99 ± 0.14	O 1s (C–O)	532.4	21.00 ± 0.64
				O 1s (O–C=O)	535.7	20.16 ± 1.74
Sample 2	0.10	C 1s	75.62 ± 1.58	O 1s (C=O)	534.3	61.76 ± 0.10
		O 1s	24.38 ± 1.58	O 1s (C–O)	532.5	24.95 ± 0.10
				O 1s (O–C=O)	535.7	13.29 ± 1.93
Sample 3	0.07	C 1s	74.46 ± 2.35	O 1s (C=O)	534.3	57.70 ± 0.32
		O 1s	25.54 ± 2.35	O 1s (C–O)	532.6	22.81 ± 0.38
				O 1s (O–C=O)	535.6	19.49 ± 0.42

Note: [a)] Data obtained by XPS analysis, per triplicate.[b)] Atomic concentration of O 1s, discriminated by functional group, after deconvolution of high resolution XPS spectra.

Table S2. Atomic ratios of O/C elements in Optilene® mesh, before and after plasma activation, at constant plasma power (500W) and time (180s), and with variable pressures.

Sample code	Pressure (mbar)	O/C ratio [a)]
Pristine iPP mesh	-	0.017 ± 0.006
Sample 1	0.20	0.266 ± 0.002
Sample 2	0.10	0.323 ± 0.028
Sample 3	0.07	0.344 ± 0.042

Note: [a)] Data obtained by XPS analysis, per triplicate.

If we compare the high resolution spectrum of C 1s for PP solid and non-porous films and that originated in the iPP mesh supported in gold substrate, without plasma discharge, slight differences can be found. Figure S1 shows the XPS deconvolution of the C 1s signal of PP samples (mesh and flat film), and holder used for measurements. The pristine Optilene® mesh (Figure S1a) presents bands at 284.3 and 285.6 eV, which have been attributed to the C–C and C–H bonds, respectively, whereas the bands at higher binding energies were assigned to C–O and C=O functional groups (at 286.5 and 288.3 eV, respectively); as

explained in the main text. Figure S1b presented bands at 285.2 and 286.7 eV, which have been attributed to the C-C\C-H and C-O bonds, respectively, in agreement with the most commonly used deconvolution reported in the literature.[4,5] However, the XPS deconvolution of the C 1s signal of the surface of the gold substrate (Figure S1c) suggested the presence of a contamination peaks (*i.e.*, adventitious carbon). Therefore, in order to calculate the atomic concentration of C and O related to our samples, the amounts of C and O coming from the substrate were subtracted accordingly. Then, Figures S1a and S1b represents uniquely the contribution of the polymer surface. All samples are related to surfaces without plasma activation.

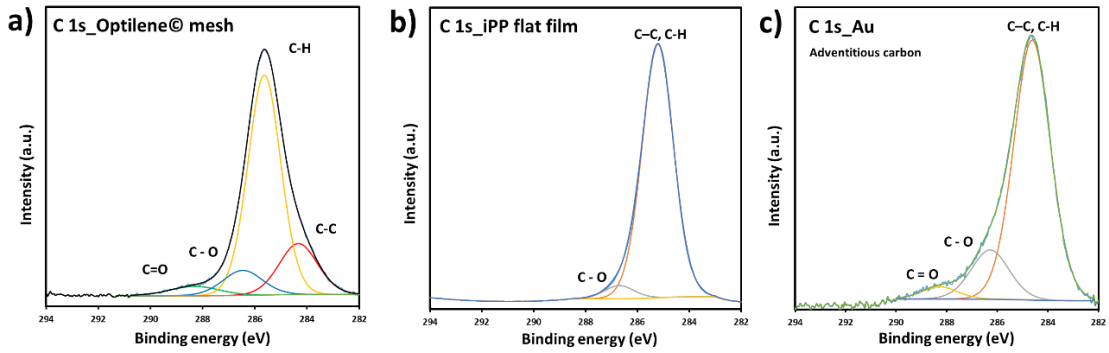

Figure S1. High-resolution XPS spectra of C1s in: a) pristine Optilene® mesh LP; b) iPP flat and non-porous film; and c) Au holder used to stick the samples.

3.3. Effect of the plasma power in the molecular structure of polypropylene meshes

Plasma-introduced functional groups that were additionally identified and qualified from FTIR and micro-Raman. Within this context, micro-Raman spectroscopy offers advantages with respect to the XPS technique. Figure S2 collects the Raman spectra used to evaluate the influence of pressure values in the chemical groups. The plasma treatment affected the absorption bands intensity, due to the surface oxidation. This is supposed to have an effect on the crystallinity and isotacticity of polymer chains, as discussed below.

At the microscopic scale, a number of indirect analytical techniques can be used to investigate the crystallinity properties of a bulk polymer, such as differential scanning calorimetry, nuclear magnetic resonance and X-ray diffraction. Crystallinity measurements on semicrystalline polymers have also been performed with vibrational spectroscopy, such as Raman or infrared, and useful data have been obtained[1,2]. Raman spectroscopy is a powerful tool for analysis of conformational arrangements of the macromolecular chains. Therefore, in this study, three sets of absorption bands were chosen to examine changes in crystallinity and isotacticity (Figure S2a). These are: (*i*) the absorption bands at 809 and 841 cm^{-1}; (*ii*) at 973 and 998 cm^{-1}; and (*iii*) at 2962 and 2953 cm^{-1}. Regarding to the first set, the band at 809 cm^{-1} is associated to the crystalline domains, reflecting changes in the C–C stretching along backbone and the rocking of CH_3 groups,[3,6,7] while the band at 841 cm^{-1} is originated by the CH_3 rocking from amorphous regions (Figure S2c).[6] These two peaks are derived from the CH_3 absorption band observed in

polypropylene melts at 830 cm^{-1}, which splits into the 809 and 841 cm^{-1} peaks when it solidifies,[1] indicating some structural changes associated with the molecular orientation of methyl groups in the PP chains. These two peaks were used to estimate the PP crystallinity (Eqs. 3 and 4). In the second set of peaks, the 973 cm^{-1} Raman shift is mainly associated to the asymmetrical stretching of the axial C–C bond and the 998 cm^{-1} peak is due to the rocking vibrational movement of the -CH_3 side group.[3,6] These two peaks have been used to evaluate the PP isotacticity (Eq. 5) and also the changes in the molecular orientation of the methyl group.[1] Finally, the last set corresponds to the absorption bands associated with the asymmetric stretching of the C–H from methyl groups (2962 and 2953 cm^{-1}) (Figure S2b) These peaks have also been related to changes in the molecular orientation of the methyl groups.[8]

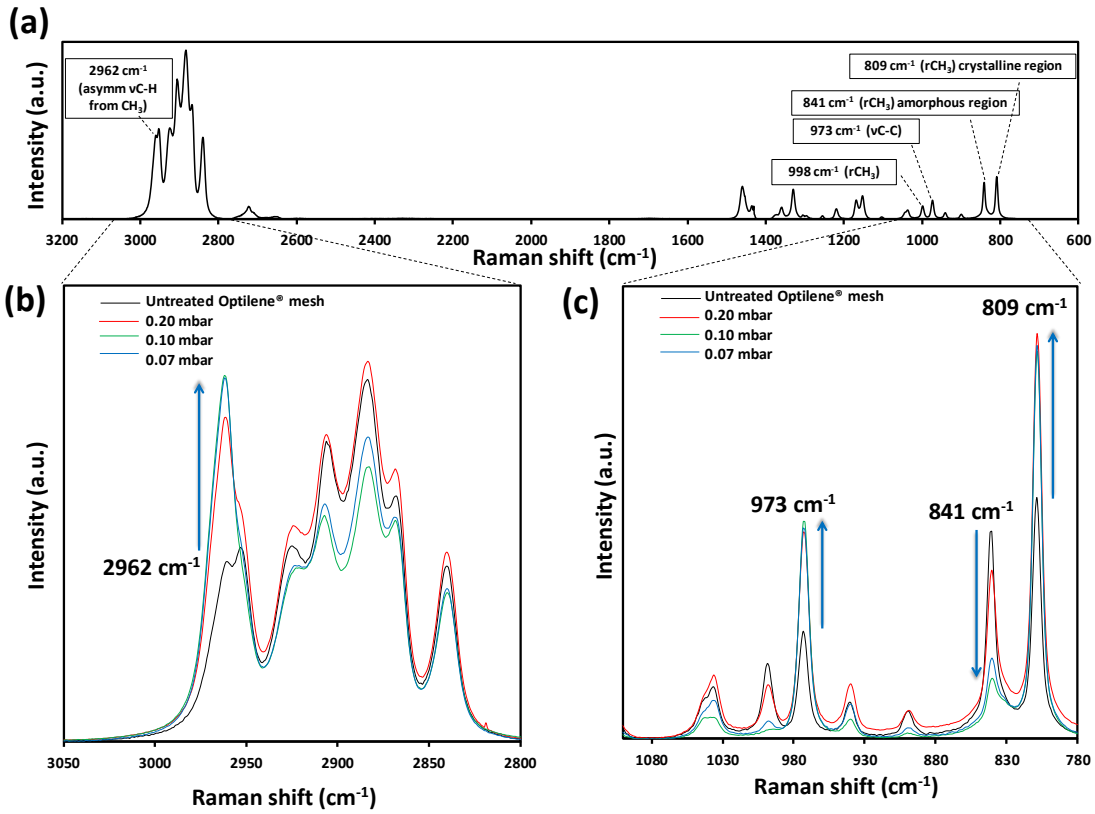

Figure S2. Raman spectra of Optilene® meshes (a) before and (b,c) after O_2-plasma surface functionalization at different purging pressure values (0.20, 0.10 and 0.07 mbar), constant plasma power (500 W), and constant plasma time (180s). (a) 3050-2800 $cm^{-1}$and (b) 1100-780 cm^{-1}. The entire spectrum is displayed in (a) for the untreated polymer, whereas the (b) 3050-2800 $cm^{-1}$and (c) 1100-780 cm^{-1} regions are shown for the plasma treated polymer.

Furthermore, the values of the isotacticity index (Table S3) dropped as the polymeric matrix was evaluated with lowering purging pressure application at the same plasma power (500 W), which is consistent with a modification of the distribution of the lateral methyl group as well as other features noticed within this study (see below). Moreover, some authors[2,9,10] revealed that the bands at 973 cm^{-1} and 1002 cm^{-1} are characteristic of the isostereoregularity of the PP matrix. The presence of peaks at 973 cm^{-1} and 1033 cm^{-1} (Figure S2) confirms that the isotacticity of the mesh after plasma activation is maintained despite a subtle reduction has been observed (Table S3). The band at 973 cm^{-1} was chosen for the isotacticity evaluation because it was found to be unaffected by the degree of crystallinity, as described previously.[1] Another important aspect observed is that reduction by twice of the plasma power (from 500 W to 250 W, at the same pressure of 0.07 mbar) does not alter the values obtained for either crystallinity or isoctaticity (Table S3).

Table S3. Cristallinity and isotacticity values calculated with the absorption bands at 809 cm^{-1}, 841 cm^{-1} and 973 cm^{-1} obtained by Raman spectroscopy for samples treated with O_2-plasma at different purging pressure and plasma power.

Sample code	**Plasma parameters (Pressure, plasma power)**	**Crystallinity (%)**	**Isotacticity**
Pristine Optilene® mesh LP	-	43.7 ± 0.15	2.24 ± 0.084
Sample 1	0.20 mbar, 500 W	58.2 ± 0.58	2.01 ± 0.028
Sample 2	0.10 mbar, 500 W	71.1 ± 0.31	1.78 ± 0.024
Sample 3	0.07 mbar, 500 W	67.3 ± 0.08	1.82 ± 0.011
Sample 4	0.07 mbar, 250 W	64.4 ± 0.86	1.85 ± 0.014

In order to understand better if the plasma functionalization is limited to the surface of the iPP meshes, Raman analyses at different depths inside the meshes were carried out. In order to improve the depth resolution, we employed the 785 nm laser that can allow us to reach about 12 µm. The spectra were recorded with regular interval of 1 µm till-10 µm. Figures S3-S6 show that no change was detected with exception of the gradual decrease of the intensity when inner part of the fibres were investigated, which was due to the variation of the Z position. Also, the crystallinity and isotacticity did not show variations when compared with the values derived from the surface spectrum.

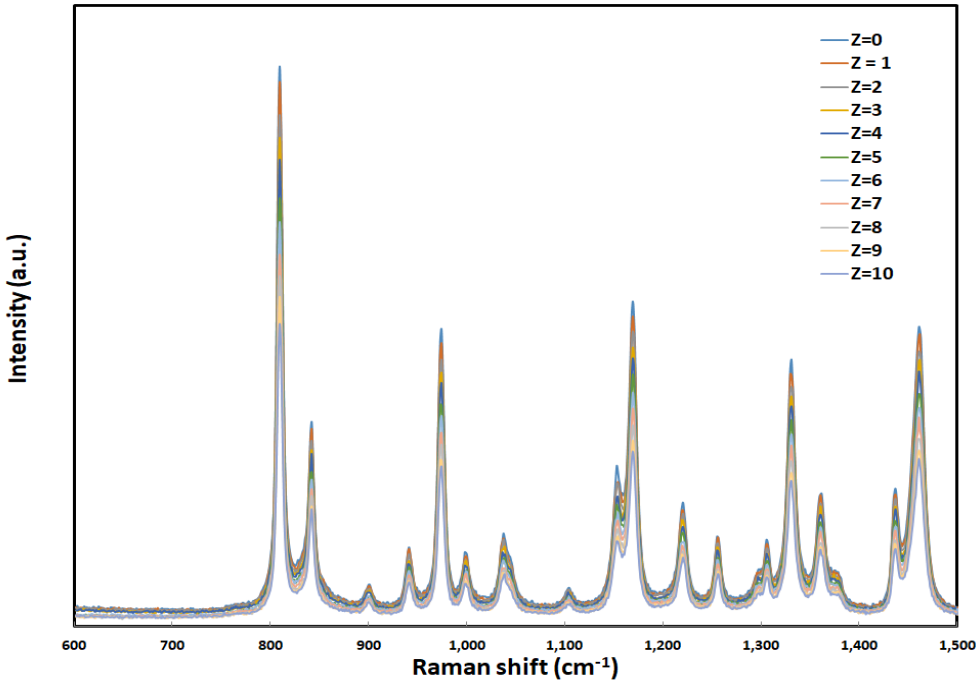

Figure S3. Raman spectra recorded by changing the Z position until a depth of 10 µm. The spectra correspond to iPP fibres treated with plasma power of 500 W and purging pressure of 0.20 mbar.

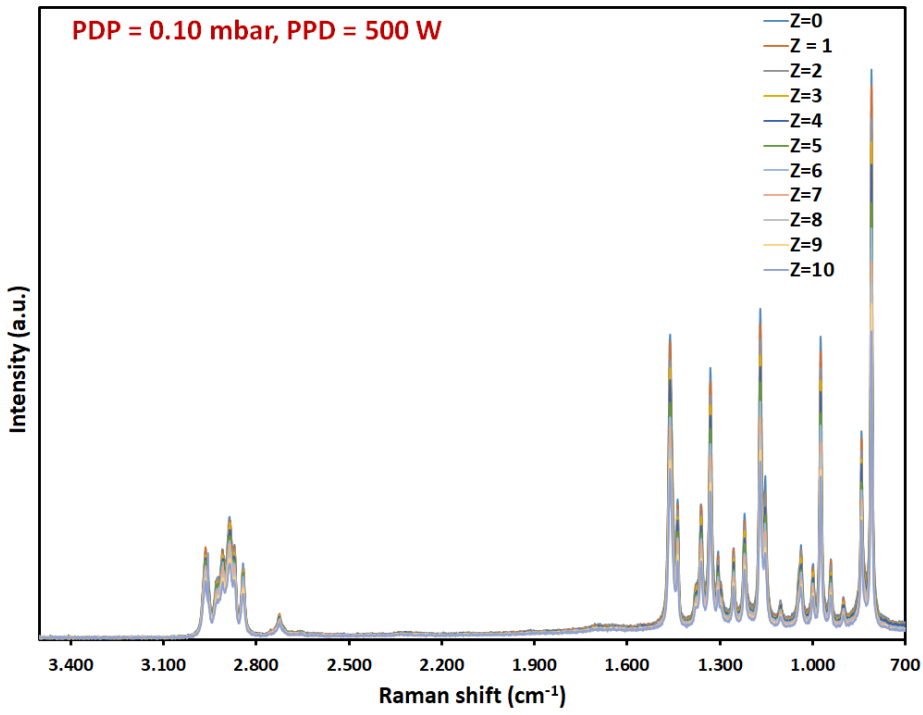

Figure S4. Raman spectra recorded by changing the Z position until a depth of 10 µm. The spectra correspond to iPP fibres treated with plasma power of 500 W and purging pressure of 0.10 mbar.

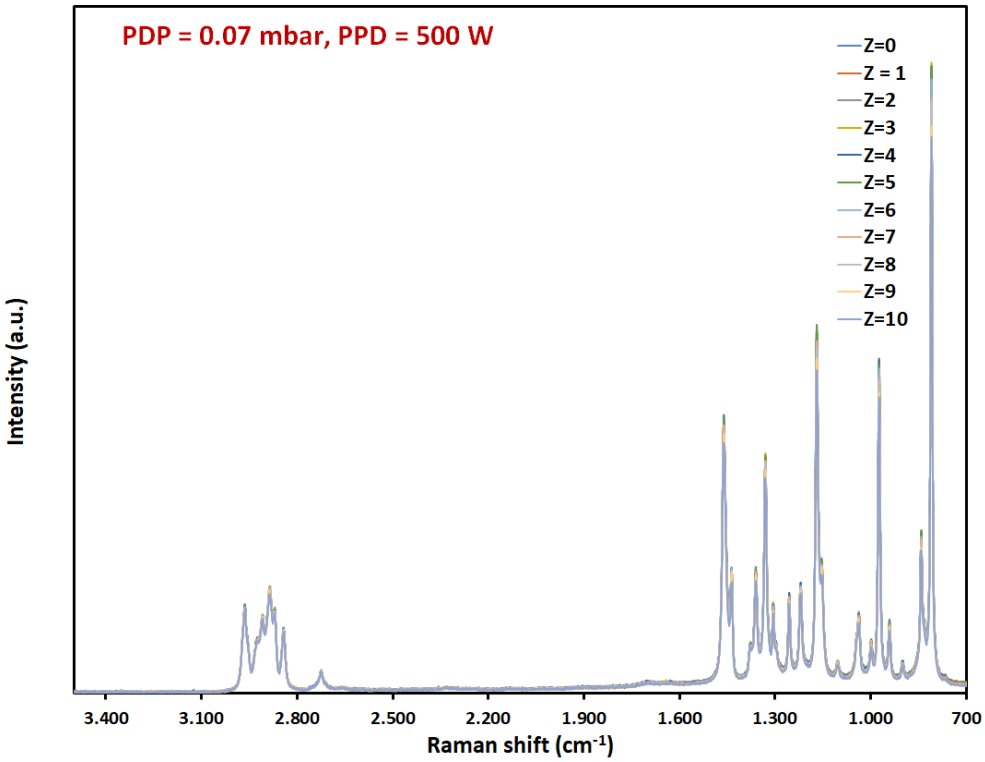

Figure S5. Raman spectra recorded by changing the Z position until a depth of 10 µm. The spectra correspond to iPP fibres treated with plasma power of 500 W and purging pressure of 0.07 mbar.

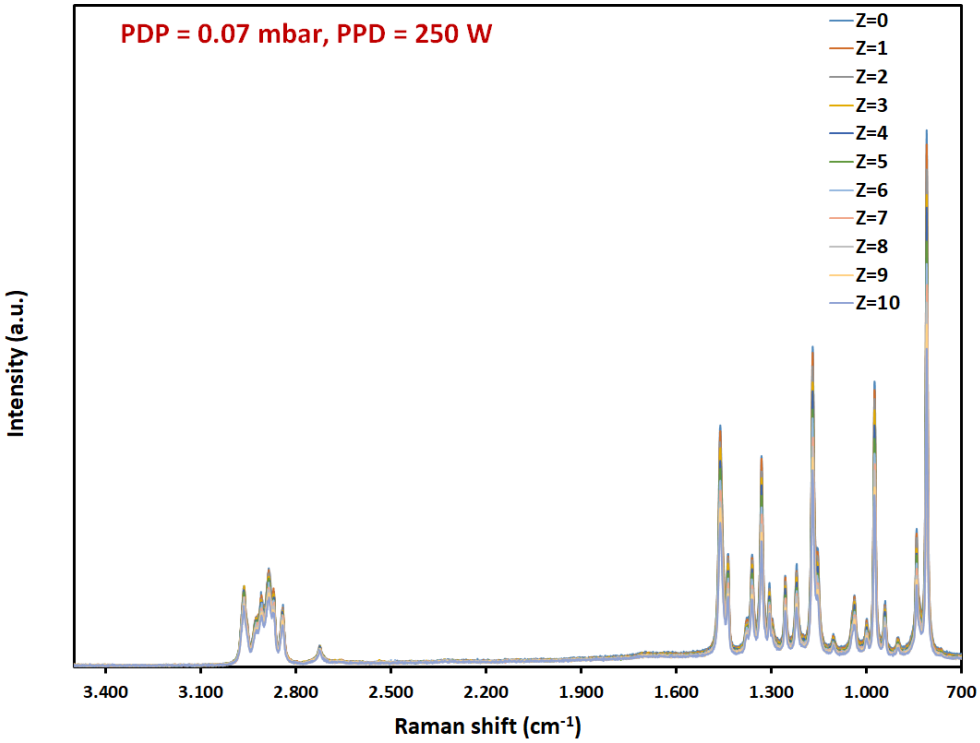

Figure S6. Raman spectra recorded by changing the Z position until a depth of 10 µm. The spectra correspond to iPP fibres treated with plasma power of 250 W and purging pressure of 0.07 mbar.

3.5. Effect of plasma functionalization in the immobilization of PNIPAAm molecules onto mesh surfaces

The surface of iPP fibres were functionalized by triplicate, at different conditions, and after plasma treatment the samples were moved to the reaction medium for NIPAAm and MBA copolymerization. Therefore, the fibre surfaces, after such treatment, was carefully investigated by FTIR and absorption bands analysed by deconvolution. Figure S7 shows the region of wavenumber related to O-H and C=O vibrations. The ratio $A_{O\text{-}H}$ / $A_{O\text{-}C=O}$ was obtained from the deconvolution of FTIR-ATR spectra.

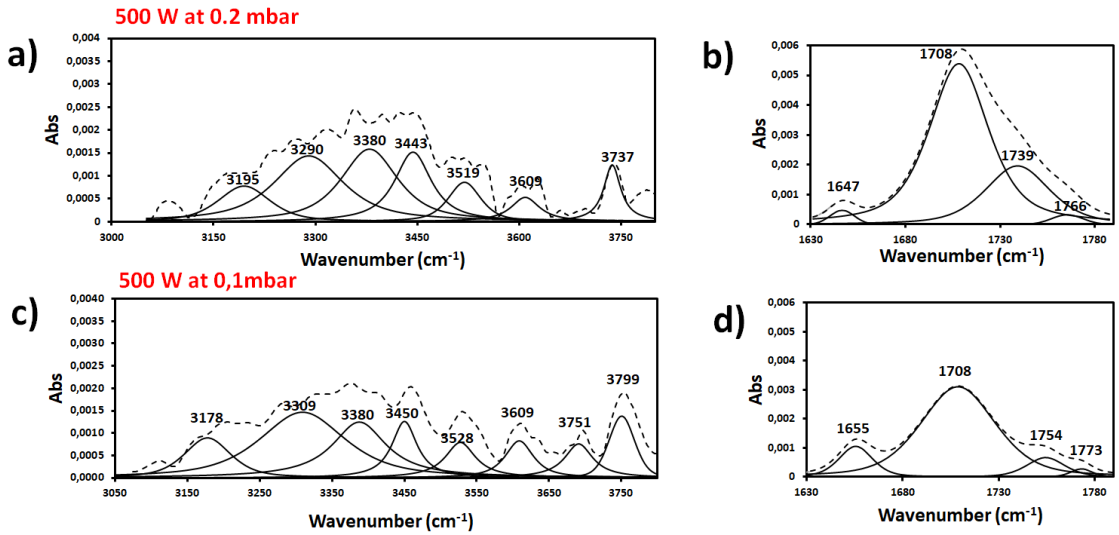

Figure S7. FTIR-ATR spectra of iPP surface after plasma activation at power discharge of 500 W and purging pressure of 0.2 and 0.1 mba. (a,c) Deconvolution of 3050-3750 cm^{-1} region (O-H stretching absorption bands), and (b,d) Deconvolution of 1630-1790 cm^{-1} region (C=O absorption bands). Dashed lines correspond to the experimental spectra, whereas continuous lines represent the deconvolution of the curves.

Table S4. Equilibrated swelling ratio (ESR) and graft yield (GY) values for iPP-*g*-PNIPAAm samples with different operative conditions.

Sample code	Plasma parameters (Pressure, plasma power)	ESR (%)	GY (mg/cm^2)
Sample 1	(0.20 mbar, 500W)	10.42 ± 2.20	1.91 ± 0.18
Sample 2	(0.10 mbar, 500W)	6.46 ± 0.19	0.50 ± 0.05
Sample 3	(0.07 mbar, 500W)	9.12 ± 0.32	0.93 ± 0.05
Sample 4	(0.07 mbar, 250W)	40.82 ± 2.34	3.89 ± 0.12

The gel composition was corroborated by FTIR and Raman spectroscopies (Figures S8a-b, respectively). Figure S8a displays characteristic absorption bands at 1640 cm^{-1} (C=O stretching of amide I), 1540 cm^{-1} (N–H bending of amide II) and 1172 cm^{-1} (C–N of amide III), while the bands assigned to the isopropyl

groups (C–$(CH_3)_2$) appear in the 1387-1367 cm^{-1} interval. The absorption band at 1459 cm^{-1} is attributed to the bending of isopropyl and methylene groups, while region comprised between 2870 and 3000 cm^{-1} corresponds to the bands associated to the C–H stretching vibrations in –CH_3 and –CH_2– groups. The broad bands in the range from 3100 to 3600 cm^{-1} with clear peaks at 3285 cm^{-1} and 3433 cm^{-1} are originated by the stretching vibrations of N–H (Amide A) and O–H (from water) groups, establishing hydrogen bonding inside the polymer backbone.[11] Interestingly, Figure S8a shows that the absorption bands of N–H and C=O groups from PNIPAAm hydrogel increase after the graft copolymerization.

On the other hand, Figure S8b, which displays the Raman spectra, evidences the presence of crosslinked PNIPAAm hydrogel onto the surface of the fibres. As it was expected, the most intense peaks are related to the PP groups, whereas polar groups from gel, like C=O (1650 cm^{-1}) appears only when the hydrogel GY is high. Then, the PNIPAAm was hardly seen by Raman spectroscopy in iPP fibres with GY of 0.50 ± 0.05 mg/cm^2 (Figure S8b, inset). Worth mentioning that the Raman spectra reported in Figure S8b were collected focusing the laser on the fibres, in the monofilament mesh.

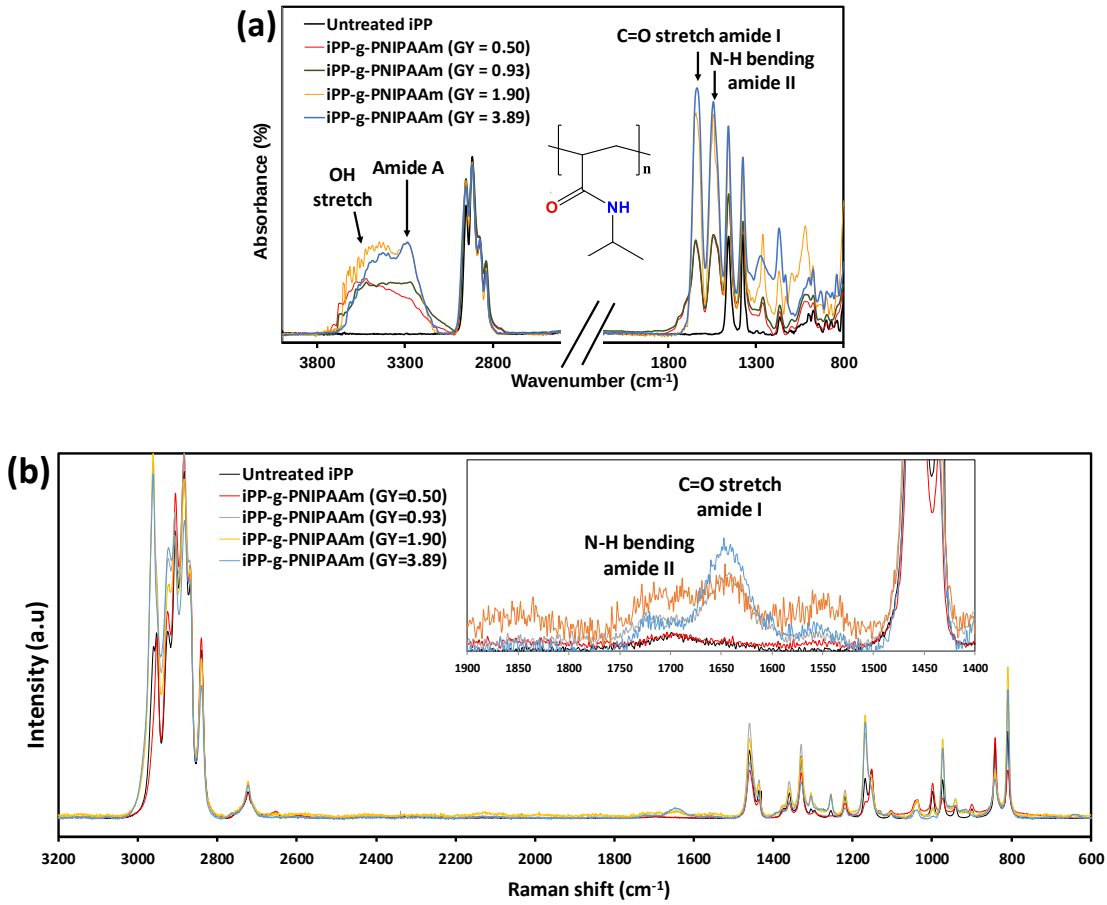

Figure S8. (a) FTIR-ATR spectra and (b) Raman spectra obtained by grafting of NIPAAm onto iPP surface, under different conditions of plasma discharge; by comparing different graft yield (GY).

In order to study the preferential orientation of gel growth, new analyses were carried out directing the Raman laser confocal microscope upon the mesh fibre and among pores. Then, samples with the highest and the lowest GY were studied: (i) purging pressure of 0.10 mbar, plasma power of 500 W, time of plasma

exposure of 180 s, and iPP-*g*-PNIPAAm with GY of 0.50 ± 0.05 mg/cm^2 (Figure S9a); and (ii) purging pressure of 0.07 mbar, plasma power of 250 W, time of plasma exposure of 180 s, and iPP-*g*-PNIPAAm with GY of 3.89 ± 0.12 mg/cm^2 (Figure 9b). As it can be seen, the spectra show important differences. In particular, the absorption bands typically found for pristine PP (section 3.2) are mainly detected above the fibres, whereas those belonging to the PNIPAAm hydrogel (C=O, 1650 cm^{-1}) were achieved above and between them. Thus, the PNIPAAm crosslinked chains grow horizontally with respect to the fibres. More specifically, when the GY is low, PNIPAAm hydrogel will be present in less quantity on the surface of the fibres than in the pores of the mesh. This observation suggests that the graft begins in the fibres functionalized by plasma and grows above and between them, establishing a soft polymer network well adhered to the monofilaments.

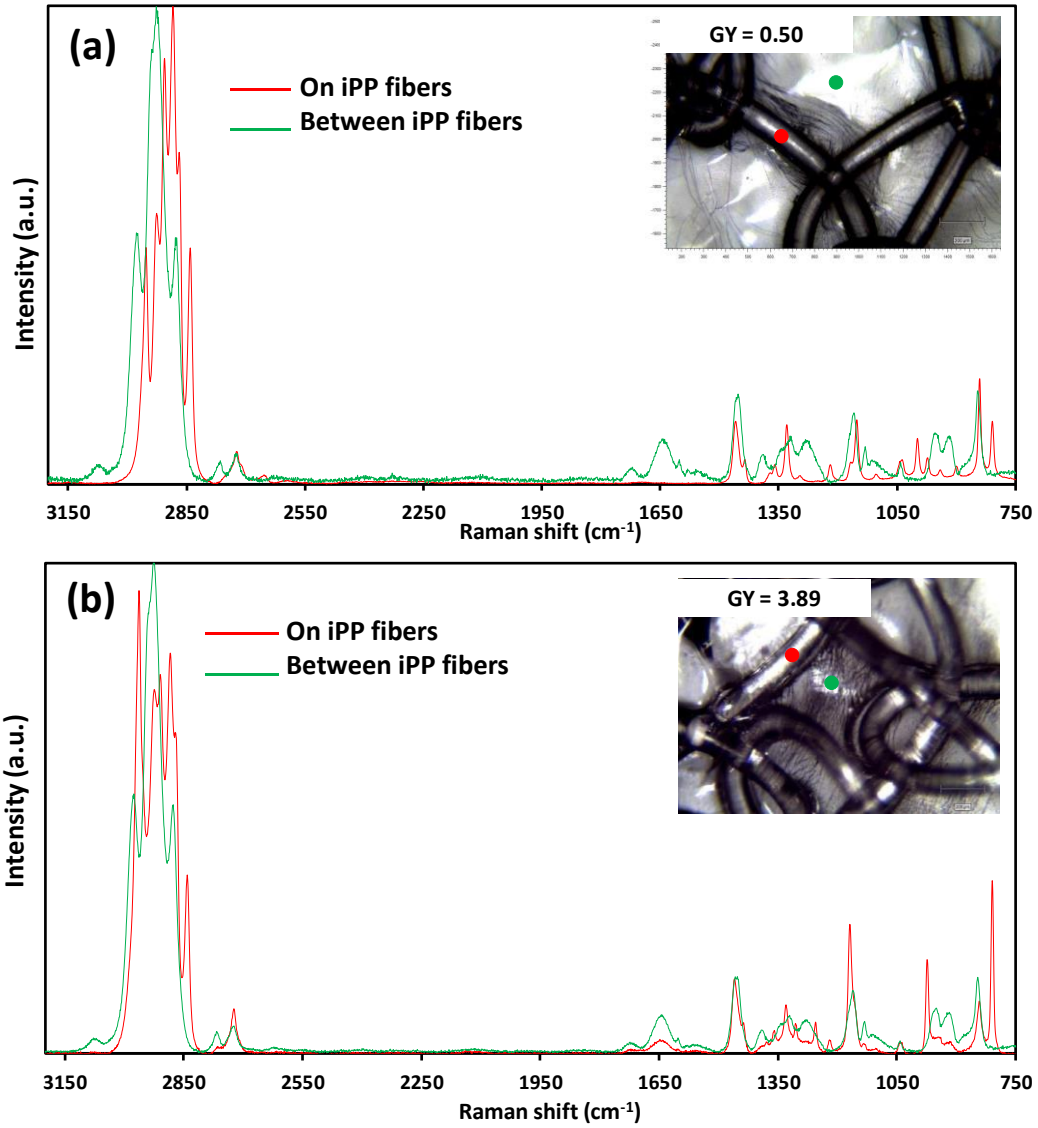

Figure S9. Raman spectra of iPP-*g*-PNIPAAm obtained under different conditions of plasma discharge: (a) lowest graft yield and (b) highest graft yield. The inset micrographs show the zones above fibres and among pores, analyzed by Raman.

References

1 C. Minogianni, K. G. Gatos and C. Galiotis, *Appl. Spectrosc.*, 2005, **59**, 1141–1147.

2 J. Martin, M. Ponçot, J. M. Hiver, P. Bourson and A. Dahoun, *J. Raman Spectrosc.*, 2013, **44**, 776–784.

3 T. Sundell, H. Fagerholm and H. Crozier, *Polymer (Guildf).*, 1996, **37**, 3227–3231.

4 Y. C. Tyan, J. Der Liao, Y. Te Wu and R. Klauser, *J. Biomater. Appl.*, 2002, **17**, 153–178.

5 S. Gorgieva, M. Modic, B. Dovgan, M. Kaisersberger-Vincek and V. Kokol, *Plasma Process. Polym.*, 2015, **12**, 237–251.

6 R. M. Khafagy, *J. Polym. Sci. Part B Polym. Phys.*, 2006, **44**, 2173–2182.

7 D. E. Gen, K. A. Prokhorov, G. Y. Nikolaeva, E. A. Sagitova, P. P. Pashinin, B. F. Shklyaruk and E. M. Antipov, *Laser Phys.*, 2011, **21**, 125–129.

8 M. Arruebarrena de Baez, P. J. Hendra and M. Judkins, *Spectrochim. Acta Part A*, 1995, **51**, 2117–2124.

9 G. Masetti, F. Cabassi and G. Zerbi, *Polymer (Guildf).*, 1980, **21**, 143–152.

10 A. 0. Ibhadon, *J. Appl. Polym. Sci.*, 1992, **46**, 2123–2129.

11 Y. Liu, W. Li, L. Hou and P. Wu, *RSC Adv.*, 2014, **4**, 24263.